

Investigation of the Changes of Fabry-Perot Fringe Patterns in Porous Silicon During Etching Process

Seunghyun Jang[†]

Abstract

Changes of Fabry-Perot fringe patterns in porous silicon during etching process has been investigated. Four porous silicon samples were prepared with four different etch currents: (a) 10 mA/cm^2 , (b) 30 mA/cm^2 , (c) 50 mA/cm^2 , (d) 100 mA/cm^2 , respectively. Optical characterization of Fabry-Perot fringe pattern on porous silicon was achieved by Ocean optics 2000 spectrometer. The change of Fabry-Perot fringes was monitored and measured during the etching process. Fabry-Perot fringes pattern start to form after couple of minutes. As the etching time increased, more reflection peaks were observed. Its full width at half maximum (FWHM) decreased rapidly when the etching time increased.

Key words : Fabry-Perot Fringe, Etching, Porous Silicon

1. Introduction

Porous silicon is a high surface area material produced by electrochemically etching single-crystal silicon in HF-containing electrolytes. It consists of a large number of interconnected Si nanocrystallites with a surface that is almost entirely covered with hydrogen atoms^[1-7].

The diameter, geometric shape, and direction of the pores depend on surface orientation, doping level and type, temperature, the composition of the etching solution, and the current density^[8,9]. Porous silicon has been employed as a large surface area matrix for immobilization of a variety of biomolecules including enzymes,⁴ DNA fragments^[10], and antibodies^[11]. Moreover, we recently showed that the electronic or optical properties of porous silicon can also be used as the transducer of biomolecular interactions, thus qualifying its utility in biosensor applications^[12,13]. A Fabry-Perot fringe pattern is created by multiple reflections of illuminated white light on the air-porous silicon layer and the porous silicon-bulk silicon interface. The induced shift in the Fabry-Perot fringe pattern caused by the change

in the refractive index of the medium upon molecular interactions of species in solution with immobilized ligands or receptors within the porous silicon matrix can be used as a sensitive method for molecular sensing.

Electrochemical etching offers both the opportunity to modulate the porosity in depth and the fabrication of structures with any refractive index profile. The thicknesses, porosities and average pore diameters of porous layers can be controlled by using parameters such as the current density, the duration of etch, cycle, and the composition of the etchant solution^[14].

Here we report the changes of Fabry-Perot fringe patterns and the values of FWHM of porous silicon prepared at different etch currents during etching process.

2. Experimental Section

2.1. Sample Preparation

Porous silicon samples were prepared by electrochemical etching of heavily doped p⁺⁺-type silicon wafers (boron doped, polished on the (100) face, resistivity of $0.8\sim1.2 \text{ m}\Omega\text{-cm}$, Siltronix, Inc.). The etching solution consisted of a 1 : 1 volume mixture of aqueous 48 % hydrofluoric acid (ACS reagent, Aldrich Chemicals) and absolute ethanol (ACS reagent, Aldrich Chemicals). The galvanostatic etch was carried out in a Teflon cell by using a two-electrode configuration with a Pt mesh counter electrode. The anodization cur-

Department of Chemistry, University of Wisconsin, Madison, 1101 University Ave., Madison, WI 53706 (USA)

[†]Corresponding author : shjang@chem.wisc.edu
(Received : January 1, 2012, Revised : March 25, 2012,
Accepted : March 27, 2012)

rent was supplied by a Keithley 2420 high-precision constant current source controlled by a computer to allow the formation of Fabry-Perot fringe patterns in porous silicon. To prevent the photogeneration of carriers, was performed the anodization in the dark. Four porous silicon samples were prepared with four different etch currents: (a) 10 mA/cm², (b) 30 mA/cm², (c) 50 mA/cm², (d) 100 mA/cm², respectively. The entire electrochemical process is carried out under constant current supplied by a computer controlled Keithley 2420 power sourcemeter.

2.2. Instrumentation and Data Acquisition

Optical reflectivity spectra are measured using a tungsten halogen lamp and an Ocean Optics S2000 CCD spectrometer fitted with a fiber optic input. The reflected light collection end of the fiber optic is positioned at the focal plane of the optical microscope.

3. Result and Discussion

PSi prepared by applying a constant current density exhibits high reflectivity in a general wide spectral region. The values of peaks in Fabry-Perot fringe spectrum satisfy the following relationship:

$$m\lambda = 2 nL \cdot \sin\theta \quad (1)$$

Where λ is the wavelength of maximum constructive interference for spectral fringe of order m, n is the index of refraction of the porous layer, and L is the thickness

of the porous layer. The optical thickness (OT) referred to as the quantity $2 nL$, was obtained from Fourier transformation (FT) of the Fabry-Perot fringe spectrum. FT arising from a sharp resonance indicated the quantity $2 nL$. The change of OT is related to the refractive index of the porous layer. The pore shape, pore size, and orientation of porous silicon layers depend on the surface orientation and doping level and type, temperature, the current density, and the composition of the etching solution. For mono-layered PSi, an anodic etch of p-type silicon wafer in ethanolic HF solution generally produced PSi single layer with a network of micropores, rather than meso- or macropores.

The pore size of p-type PSi can be increased by increasing the concentration of the dopant and decreasing the aqueous HF concentration. High current densities resulted in the desired well-defined cylindrical macropores, rather than the random orientation of highly interconnected micropores.

The PSi etched with 10 mA/cm² of current density for five min. displayed Fabry-Perot fringes in the optical reflective spectra shown in Fig. 1. The change of Fabry-Perot fringes was monitored and measured at every one minute during the etching process. After one minute etching, single broad reflection peak whose full width at half maximum (FWHM) of 125 nm was appeared at around 500 nm indicating that the optical thickness of porous silicon at this point was 500 nm. Fabry-Perot fringes pattern start to form after two minutes. Three reflection resonances in reflection spectra in two minutes appeared at 700, 550, and 490 nm, respectively. As

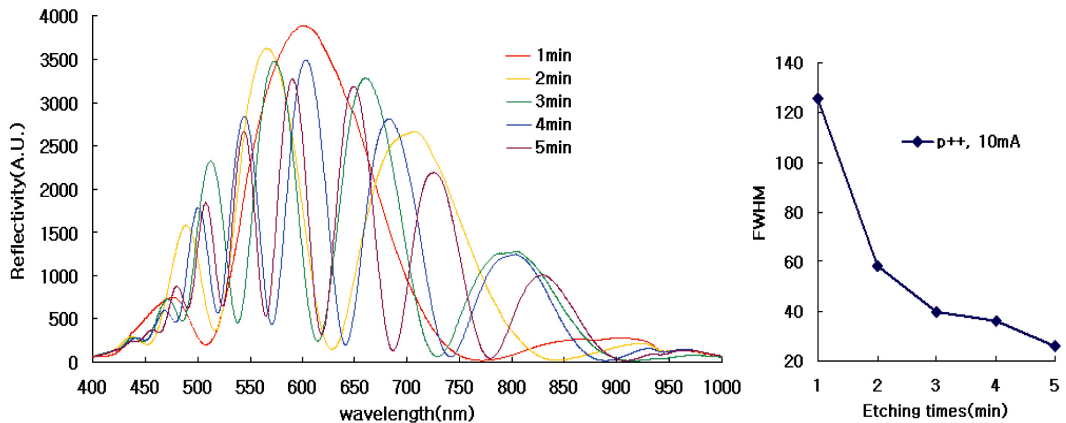


Fig. 1. Fabry-Perot fringe patterns in reflection spectra and a plot of full width at half maximum profile during the etching with 10 mA/cm² of current density.

the etching time increased, more reflection peaks were observed. FWHM decreased rapidly when the etching time increased.

Fig. 2 showed Fabry-Perot fringe patterns in reflection spectra and a plot of full width at half maximum profile during the etching with 30 mA/cm^2 of current density. After one min. etching, four reflection resonances in reflection spectra were already formed which indicated that Fabry-Perot fringe patterns start to form before one minute. As the etching time increased, more reflection peaks were observed. When the etching times were constant, more number of reflection peaks were formed compare to the porous silicon obtained with lower current density. FWHM decreased from 50 to 10 nm as an etching time increased.

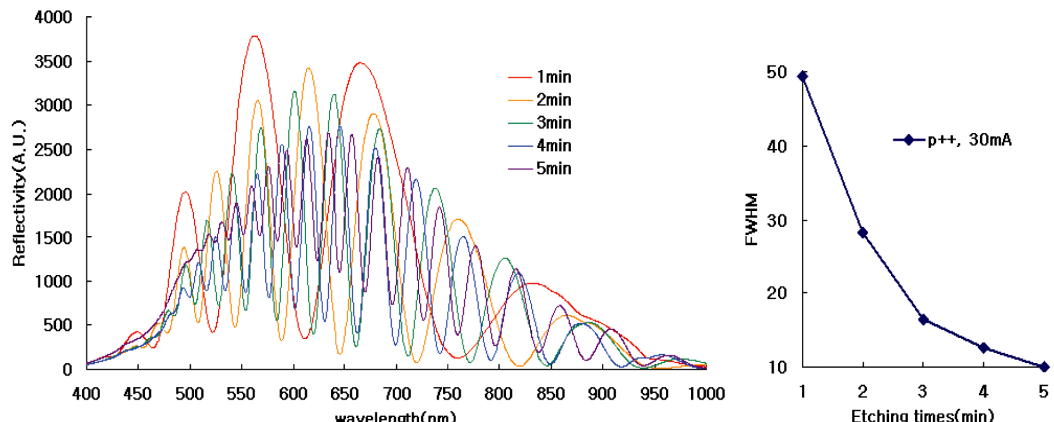


Fig. 2. Fabry-Perot fringe patterns in reflection spectra and a plot of full width at half maximum profile during the etching with 30 mA/cm^2 of current density.

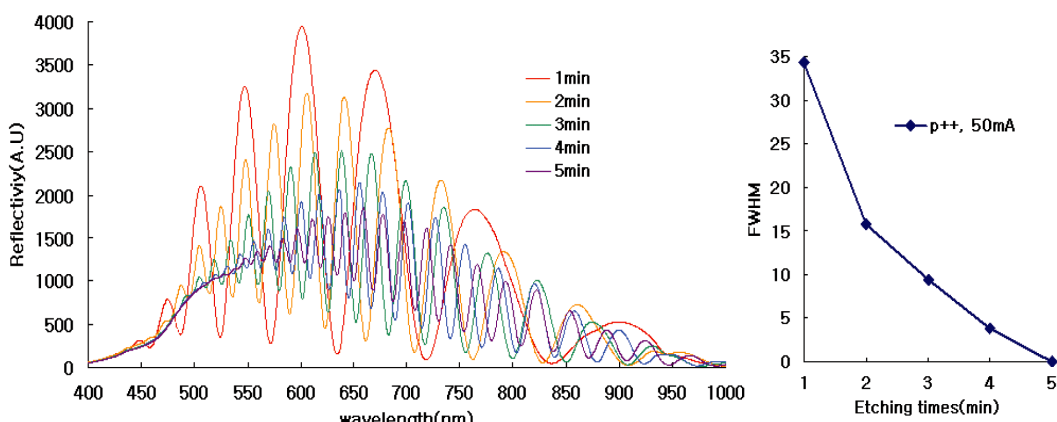


Fig. 3. Fabry-Perot fringe patterns in reflection spectra and a plot of full width at half maximum profile during the etching with 50 mA/cm^2 of current density.

Fig. 3 showed Fabry-Perot fringe patterns in reflection spectra and a plot of full width at half maximum profile during the etching with 50 mA/cm^2 of current density. The change of Fabry-Perot fringe patterns and decrease of FWHM were similar to that observed from the previous samples. Fabry-Perot fringe patterns were not clearly formed after 5 minutes of etching.

Fig. 4 showed Fabry-Perot fringe patterns in reflection spectra and a plot of full width at half maximum profile during the etching with 100 mA/cm^2 of current density. The change of Fabry-Perot fringe patterns and decrease of FWHM were also similar to that observed from the previous samples. As the etching time increased, more reflection peaks were observed. However, the deformation of Fabry-Perot fringe patterns were observed

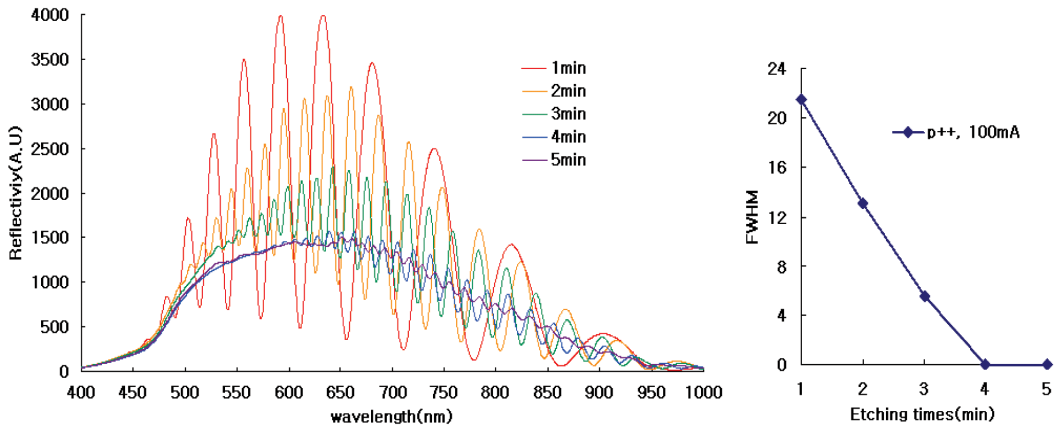


Fig. 4. Fabry-Perot fringe patterns in reflection spectra and a plot of full width at half maximum profile during the etching with 100 mA/cm^2 of current density.

after 3 minutes of etching. This result indicated that the deformation of Fabry-Perot fringe patterns took place earlier and FWHM decreased at higher current density. The deformation of Fabry-Perot fringe patterns might be the indication of destruction of porous layer.

4. Conclusion

Changes of Fabry-Perot fringe patterns and FWHM in porous silicon during etching process has been investigated with four porous silicon samples prepared at different etch currents. The change of Fabry-Perot fringe patterns and decrease of FWHM displayed similar tendency for all samples. As the etching time increased, more reflection peaks were observed. FWHM decreased rapidly when the etching time increased. The deformation of Fabry-Perot fringe patterns took place at higher current density. This deformation of Fabry-Perot fringe patterns might be the indication of destruction of porous layer due to high current density during the etching process.

References

- [1] P. Gupta, V. L. Colvin, and S. M. George, "Hydrogen desorption kinetics from monohydride and dihydride species on silicon surfaces", *Phys. Rev. B*, Vol. 37, p. 8234, 1988.
- [2] P. Gupta, A. C. Dillon, A. S. Bracker, and S. M. George, "FTIR studies of H₂O and D₂O decomposition on porous silicon surfaces", *Surf. Sci.*, Vol. 245, p. 360, 1991.
- [3] Y. J. Chabal, "Infrared spectroscopy of semiconductor surfaces: H-terminated silicon surfaces", *J. Mol. Struct.*, Vol. 292, p. 65, 1993.
- [4] L. T. Canham, "Silicon quantum wire array fabrication by electrochemical and chemical dissolution of wafers", *Appl. Phys. Lett.*, Vol. 57, p. 1046, 1990.
- [5] A. G. Cullis and L. T. Canham, "Visible light emission due to quantum size effects in highly porous crystalline silicon", *Nature*, Vol. 353, p. 335, 1991.
- [6] K. J. Nash, P. D. J. Calcott, L. T. Canham, and M. J. Kane, "The origin of efficient luminescence in highly porous silicon", *J. Luminesc.*, Vol. 60-61, p. 297, 1994.
- [7] J. L. Heinrich, C. L. Curtis, G. M. Credo, K. L. Kavanagh, and M. J. Sailor, "Luminescent colloidal silicon suspensions from porous silicon", *Science*, Vol. 255, p. 66, 1992.
- [8] R. L. Smith and S. D. Collins, "Porous silicon formation mechanisms", *J. Appl. Phys.*, Vol. 71, R. 1, 1992.
- [9] P. C. Searson, "Advances in Electrochemical Sciences and Engineering", VCH: Mannheim, Germany, p. 69, 1994.
- [10] J. Drott, K. Lindstrom, L. Rosengren, and T. Laurell, "Porous silicon as the carrier matrix in microstructured enzyme reactors yielding high enzyme activities", *J. Micromech. Microeng.*, Vol. 7, p. 14, 1997.
- [11] K. L. Beattie, W. G. Beattie, L. Meng, S. L. Turner, R. Coral-Vazquez, D. D. Smith, P. M. McIntyre, and D. D. Dao, "Advances in genosensor research", *Clin. Chem.*, Vol. 41, p. 700, 1995.
- [12] T. Laurell, J. Drott, L. Rosengren, and K. Lind-

- strom, "Enhanced enzyme activity in silicon integrated enzyme reactors utilizing porous silicon as the coupling matrix", *Sens. Actuators, B*, Vol. 31, p. 161, 1996.
- [13] V. S. Y. Lin, K. Motesharei, K. P. S. Dancil, M. J. Sailor, and M. R. Ghadiri, "A porous silicon-based optical interferometric biosensor", *Science*, Vol. 278, p. 840, 1997.
- [14] M. J. Sailor, "Properties of porous silicon", Datareview Ser. No. 18, Canham: London, p. 364, 1997.